Computational Study of the Structural and Electronic Properties of Dopant Ions in Microporous AlPOs. 1. Acid Catalytic Activity of Divalent Metal Ions

Iman Saadoune,* Furio Corà, and C. Richard A. Catlow

Davy Faraday Research Laboratory, The Royal Institution of Great Britain 21 Albermarle St., London W1S 4BS, U.K.

Received: October 23, 2002

Periodic ab initio QM calculations are applied to study the structure and acidity of Mg, Ca, Cr, Mn, Fe, Co, Ni, Zn, and Sr divalent metal ions in the AlPO-34 framework, charge compensated by an acid proton on a neighboring oxygen. Our results show that the local environment of the divalent dopants is a distorted tetrahedron, in which the $Me-O_H$ bond of the dopant to the protonated oxygen is ∼0.15 Å longer than the other three Me−O bonds. The nature of bonding between the Me^{2+} dopants and the neighboring oxygens is ionic in nature, explaining the Lewis acidity of the Me^{2+} ions. However, for Ni^{2+}, the Lewis active orbitals are oriented within the framework, where they are screened from an effective Lewis- type interaction with adsorbed molecules. The attack of Lewis bases is favored from the side of the framework opposite to the Brønsted acid proton. The replacement energy of a framework Al^{3+} with a Me^{2+} ion increases linearly as a function of the ionic size of Me^{2+}. Finally, we show that the acid strength is attributable to a complex combination of the structural and electronic features of the dopant ion and does not show appreciable correlation with the local environment or electronic distribution of the Me^{2+} dopant in the framework.

1. Introduction

Microporous oxides, whose interstices have dimensions comparable to simple organic molecules, are highly selective heterogeneous catalysts.[1] This feature is linked to the confined environment provided by the porous framework to the catalytically active sites, which can be reached in the micropores only by selected molecules or parts of molecules. Even small modifications of the framework structure may change the accessibility of the active sites and, therefore, alter dramatically the catalytic properties.[2]

Since the discovery by Weisz et al of H-ZSM-5 as a powerful solid acid catalyst for the shape-selective dehydration of methanol to useful hydrocarbons,[3,4] intensive research in the field of microporous oxides, resulted in the synthesis of microporous solids with exceptional structural and chemical diversity. This success has been achieved partly by a better understanding of the synthesis procedure, a topic which more recently has benefited from the atomic-level detail gained in computer modeling studies[5−7] but also because of the growing range of chemical building blocks from which microporous oxides can now be composed. Indeed, the original family of aluminosilicates and silica-based zeolites has been extended to include aluminophosphates (AlPOs) and gallophosphates (GaPOs), as well as metal modified versions of these compounds (MeAPOs),[1] all generically indicated under the common name of "zeotypes". In this paper, we are particularly interested in the chemistry of microporous AlPOs that consist of corner-shared AlO_4 and PO_4 tetrahedra, which build up a neutral three-dimensional framework with channels and pores of molecular dimensions. AlPOs are structurally analogous to the class of aluminosilicate zeolites, from which they can be obtained by replacing pairs of Si^{4+} ions with alternating Al^{3+} and P^{5+} ions.

Despite the structural analogy, AlPOs show a greater flexibility than zeolites toward chemical substitutions. The formal charge of dopants successfully introduced in the framework of AlPOs varies between +2 to +5.[8] As a general rule, metal dopants with formal charge of +2 and +3 replace Al, whereas +4 and +5 ions replace the P ions of the framework. The inclusion of dopants has been shown to confer either acid and/or redox activity to the microporous materials.[9,10,11] Brønsted acidity is introduced in AlPOs when acid protons charge-compensate the presence of low valence metal ions in the framework, such as the divalent Mg^{2+}, Co^{2+}, Fe^{2+}, or Ni^{2+} ions replacing for Al^{3+} or Si^{4+} replacing for P^{5+}. In addition, MeAlPOs show Lewis acidity associated with the metal dopants in the AlPO framework.[12]

Among the acid catalyzed reactions, three are of particular interest, namely, (1) the conversion of methanol to light olefins, such as ethylene, propene, and butene, which are the centerpiece in the production of synthetic fibers, plastics, and petrochemicals; (2) the skeletal isomerization of alkenes into their branched chain analogues, an example of which is provided by the isomerization of butene to isobutene, a starting material for the production of methyl *tert*-butyl ether (MTBE), used as an oxygenated octane additive in the reformulated gasolines; and (3) the catalytic cracking in the oil refining industry.

Metal-doped aluminophosphate molecular sieves are among the microporous heterogeneous catalysts active for these three catalytic reactions.[13−15] The acid strength and catalytic activity, however, depend on the type of metal dopant employed. Several recent experimental publications have investigated the correlation between acidity, the local structure of the active site, and nature of the metal dopant in AlPOs.[16−18]

Apart from the acid acitivity, the MeAlPO catalysts doped with transition metal ions play a prominent role in selective oxidation reactions of hydrocarbons.[19] Redox activity in MeAlPOs is instead achieved when the transition metal dopants in

* To whom correspondence should be addressed. E-mail: iman@ri.ac.uk.

10.1021/jp027285h CCC: $25.00
Published on Web 03/12/2003

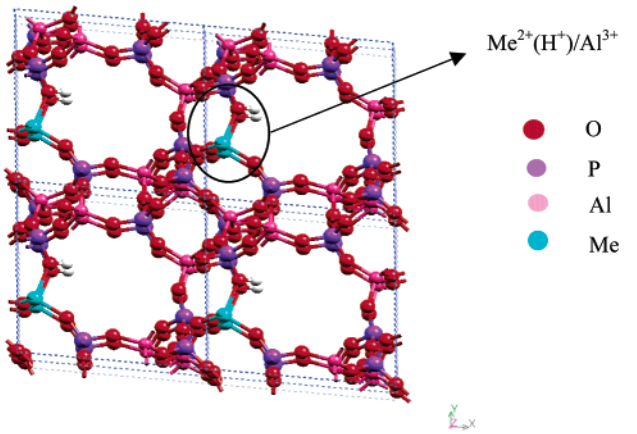

Figure 1. Representation of a Me^{2+} substitutional ion, charge-compensated by an acidic proton, in the AlPO-34 framework described with a supercell model.

the framework, such as Cr, Mn, Fe, or Co, can reversibly change their oxidation state. Understanding the structural, acid, and redox properties of the active sites associated with different metal ions in AlPOs is clearly therefore necessary for controlling the activity and selectivity of MeAlPO catalysts.

To investigate how the catalytic properties of MeAlPOs depend on the type of metal dopant, we have undertaken an extensive computational study, based on periodic ab initio quantum-mechanical (QM) methods, the aim of which is to investigate the structural and electronic properties for a range of 2+ and 3+ cations in AlPO frameworks. In this paper, we present results on low-valent metal dopants in the AlPO-34 framework, charge-balanced by a proton on one neighboring oxygen, and we shall consider the Brønsted acid strength of the doped framework. We also employ the results of QM calculations to investigate possible correlations between the acidity of the doped framework and the atomic properties of the dopant, such as ionic radius and electronegativity, and its crystalline environment (bond distances and angles) in the AlPO framework. Results concerning trivalent metal doped AlPO-34 and the behavior of redox active transition metal ions, are reported in a subsequent paper.[20]

2. Computational Details

In our work, we consider the isomorphous substitution of several low-valent metal ions in the AlPO-34 framework, shown in Figure 1, chosen as representative of the class of microporous AlPO catalysts. The AlPO-34 polymorph is isostructural to the aluminosilicate zeolite Chabasite. We have chosen this particular framework type, because of the relevance of AlPO-34 and its metal-doped derivatives to catalysis, coupled with the limited dimensions of its unit cell (6 $AlPO_4$ formula units, or 36 atoms for the undoped material), which makes its study feasible on a routine scale with accurate QM calculations. We have used the supercell approach, where the doped framework of MeAlPO-34 is described using periodic boundary conditions. The level of doping used in our calculations is of one dopant per unit cell of the host AlPO-34 framework. Although the supercell approach is computationally expensive, it provides us with a correct description of the crystalline environment, including the Madelung field and the structural strain caused by the crystalline matrix on the substitutional defect.

We have investigated the chemistry that follows doping of the AlPO-34 framework with acid-active divalent ions, namely, Mg, Ca, Sr, Cr, Mn, Fe, Co, Ni, and Zn, in the Al framework site. Each low-valent dopant is charge-compensated by protonating one of its four nearest neighbor oxygen ions in the framework.

The calculations are performed at the (unrestricted) Hartree−Fock (HF) level of theory, as implemented in the latest version of the program CRYSTAL.[21] The electronic distribution of the system is described as a linear combination of atomic orbitals, and the basis functions are expressed analytically as a contraction of Gaussian-type orbitals. The basis set employed to describe the host AlPO framework has recently been optimized by Corà et al;[22] it is of a double-ζ plus polarization quality, which allows for a good description of the electronic distribution on the metal sites. The basis sets used for the divalent dopants are taken from the CRYSTAL code on-line library.[23] For Mg^{2+}, Ca^{2+}, and Ni^{2+} ions, we used 8-511d1G, 86-511d3G, and 86-411d31G basis sets respectively, while all of the other metal dopants are described by a 86-4111d41G basis set. The basis set used for Sr^{2+} is previously unpublished and is given as supplementary information.[24] We used the HF Hamiltonian in our work because it includes the exact expression for the exchange forces, which are expected to be important for the description of the spin state of open-shell transition metal ions. The HF calculations on the undoped framework yielded an equilibrium structure in very close agreement with experiment;[22,25] we expect therefore the results of HF calculations on the doped systems to provide us with a reliable description of the local environment of the metal ions that can be usefully compared with experimental data, for instance from X-ray absorption spectroscopy.[26]

The truncation of the Coulomb and exchange interactions are achieved in CRYSTAL by selecting a series of overlap "cutoffs". We have used the values of (5,5,5,5,11); outside this threshold, integrals are disregarded or evaluated by Ewald summations. The sampling of reciprocal space has been performed in a regular array of $2 \times 2 \times 2$ k points, which for wide band-gap insulators such as AlPOs is sufficient to converge results.

Our calculations on substitutional metal ions have been performed using a two step procedure: first relaxing the AlPO framework around the dopant with methods based on interatomic potentials (IP) and subsequently refining the local structure around the dopant ion with periodic ab initio calculations.

The force field that we used in the first step is the shell model potential of Gale and Henson,[27] derived for undoped AlPOs. We obtained the interaction parameters between the different dopant ions and oxygen (Me−O) by systematically changing the Al−O parameters, so that they represent a new metal ion of approximately the correct ionic radius.[28] The optimization of the AlPO structure with the IP method allows the expansion of the unit cell parameters, needed to accommodate the steric strain caused by the greater size of the dopant ions.

The energy minimized structure of the doped framework from the IP work, is then refined with periodic QM calculations, in which no constraint is imposed onto the electronic configurations of the metal dopants under investigation, except for their spin multiplicity. For the dopant ions with open shell electronic configuration, namely, Cr^{2+} ($3d^4$), Mn^{2+} ($3d^5$), Fe^{2+} ($3d^6$), Co^{2+} ($3d^7$), and Ni^{2+} ($3d^8$), we have investigated all of the possible spin states compatible with the number of d electrons. The relative stability of the different spin states has been compared by calculating their energy in the geometry generated by the IP calculation. Our calculations suggest that the high spin state is stable for all of the metal ions studied. We attribute this result to the low crystal field splitting in the AlPO framework, which is expected for divalent ions of the first transition series that

are tetrahedrally coordinated by oxygens. All of the HF calculations reported in the following discussion are therefore based on transition metal ions in a high spin configuration.

At the level of doping chosen, i.e., of one dopant ion per unit cell, the metal dopants are separated by a distance equal to the unit cell dimension of the host framework (approximately 10 Å; see Figure 1), for which the spin interaction among dopants with unpaired electrons can be considered as negligible. All our calculations have therefore been performed with a ferromagnetic order, in which all the transition metal ions have parallel spin, as this minimizes the computational cost.

For each dopant examined, we have performed a geometry optimization at the QM level; these calculations included all of the internal coordinates, but not the lattice parameters, which have been kept fixed at their value optimized in the IP study. The version of the CRYSTAL code employed in our calculations includes the analytical evaluation of forces,[29,30] which has been exploited in the geometry optimization. All of the calculations have been performed using P1 symmetry.

Once the equilibrium structure has been obtained, we have calculated numerically the dynamical matrix at the Γ point of reciprocal space. Diagonalization of the dynamical matrix yields the phonon spectrum of the system, in the harmonic approximation, from which we have derived the OH stretching frequencies reported in section 3.

From the periodic QM calculations performed, we can obtain direct quantitative information about the electronic properties and the local structural environment of metal dopants in the AlPO lattice and the energy of the doped MeAlPO framework. The calculated energy for perfect and Me-doped frameworks can be combined to estimate the energetics of substitution of the Me ions in the microporous AlPO framework. Because the synthesis of MeAlPOs is performed in an aqueous medium, by hydrothermal synthesis,[31,32] we shall consider as suitable reference states for the divalent metal ions outside the framework, their hexa-aqua complexes, $[Me(H_2O)_6]^{2+}$, whereas the $[Al(H_2O)_5(OH)]^{2+}$ complex is used to represent the Al ions. Of course, this approach is an approximation, as only the first solvation sphere of the ions is included; nonetheless, it represents a suitably simple computational model of the solvated ions. In the paper, we shall therefore calculate the replacement energy of the di-valent Me dopants for an Al^{3+} ion in the AlPO framework according to the following equations:

$$\text{ALPO}-34 + [Me^{II}(H_2O)_6]^{2+} \xrightarrow{\Delta E_{II}} Me^{II}\text{HAlPO-34} + [Al(H_2O)_5(OH)]^{2+} \quad (1)$$

$$\Delta E_{II} = [E[Al(H_2O)_5(OH)]^{2+} + E(Me^{II}\text{HAlPO-34})] - [E(\text{ALPO-34}) + E[Me^{II}(H_2O)_6]^{2+}] \quad (2)$$

The relative values of the replacement energies ΔE_{II} indicate the relative ease of inclusion of the dopant in the AlPO framework and also the stability of the doped MeAlPO material.

To obtain the replacement energies ΔE_{II}, we have optimized the structure and calculated the energy of the molecular species with a set of computational parameters consistent to that employed for the perfect and defective solids. Details of the molecular calculations performed are discussed elsewhere.[20] As for the open-shell transition metal ions in the AlPO-34 framework, we have optimized all possible spin states compatible with the number of d electrons. Also in the molecular complexes, our calculations found that all of the transition metal ions studied in this work are stable in the highest spin state, because of the relatively low ligand field splitting of the Me-*d* levels caused by the water ligands in the gas-phase-like $Me(H_2O)_6$ complexes.

TABLE 1: Me−O Bond Distances *R*, in Å, for Divalent Metal Dopants in the MeAlPO-34 Acid Catalysts Examined[a]

Me	R(Me−O_1)	R(Me−O_2)	R(Me−O_3)	R(Me−O_H)	$\langle R\rangle$	exp
Mg	1.85	1.87	1.91	2.08	1.93	1.94[50]
Ca	2.17	2.19	2.24	2.41	2.25	
Cr	1.99	2.03	2.04	2.36	2.11	
Mn	2.01	2.02	2.04	2.26	2.08	2.02[35]
Fe	1.97	1.98	1.99	2.19	2.01	
Co	1.94	1.94	1.95	2.14	1.99	1.94[51]
Ni	1.89	1.89	1.90	2.19	1.97	1.94[52]
Zn	1.90	1.90	1.91	2.19	1.97	1.96[53]
Sr	2.36	2.42	2.45	2.55	2.44	
Al	1.72	1.72	1.73	1.73	1.73	1.73[54]

[a] Oxygens labeled 1−3 are in order of increasing distance from the Me dopant, O_H is the protonated oxygen of the Brønsted acid group. The column indicated as $\langle R\rangle$ reports the average Me−O bond distance. The Al−O bond distances in the undoped AlPO-34 framework are reported, for comparison. Experimental EXAFS or crystallographic data from the literature, where available, are also reported.

TABLE 2: Calculated Value of the T−O−P Angles in the MeAlPO-34 Frameworks[a]

Me	Me−O_H−P	Me−O_{nn}−P	(T−O−P)	(Al−O−P)
Mg	132.41	138.69	147.17	148.86
Ca	126.05	127.84	142.61	144.96
Cr	127.50	124.89	143.92	147.72
Mn	127.81	130.91	145.06	147.89
Fe	128.97	131.93	145.77	148.54
Co	129.34	133.79	146.06	148.51
Ni	126.44	135.56	146.41	148.58
Zn	131.30	132.47	145.73	148.38
Sr	116.20	118.14	140.49	144.96
Al	148.59	148.59	148.59	148.59

[a] The symbol Me−O_H−P indicates the angle around the bridging hydroxyl group, Me-O_{nn}-P is the average of the four angles on the oxygens that are nearest nighbour to the dopant, while the column T−O−P indicates the values of the angle averaged over the whole structure. The column Al−O−P refers to the angle around all oxygen ions in the structure, that are not nearest neighbor to the dopant.

3. Results

We now present the results of our calculations, reporting separately the structural details, electronic properties, energetics, and acid strength of the different MeAlPO-34 materials investigated.

3.1. Local Environment of the Divalent Metal Dopants. The structural parameters that describe the local environment of the Me^{2+} dopants in AlPO-34, as obtained from our QM structural optimization and from experimental data where available, are summarized in Tables 1 and 2. These include the four Me−O bond distances, R(Me−O_n), between the Me dopant and its four nearest neighbor oxygens; the average Me−O bond distance, $\langle R\rangle$; and the Me−O−P angles around the oxygens that are nearest neighbors of the metal. We also report the value of the T−O−P angle (T = Me and Al), averaged over all of the oxygen ions of the structure. Here and in the following discussion, we shall use the following labeling of the four oxygens that are nearest neighbors to the dopant: O_H is the protonated oxygen, whereas O_{1-3} are the three not protonated ones, in order of increasing distance from Me^{2+}.

From the calculated Me−O bond distances reported in Table 1, we see that the local environment of all of the divalent dopants is a very distorted tetrahedron, which is true not only for the

open-shell ions but also for the closed-shell dopants such as Mg^{2+}, Ca^{2+}, and Sr^{2+}. The structural distortion is dictated by the nonchemical equivalence of the four nearest-neighbor oxygens of the Me ion, caused by the presence of the acid proton bonded to one oxygen. Jahn−Teller type distortions, if present, play only a minor role compared to the relaxation around the acid OH group. The longest Me−O bond is the one to the protonated oxygen, a result which is consistent with the Al^{3+}/Si^{4+} defect in aluminosilicate zeolites, where several computational studies have shown that the Al−O_H bond distance is considerably longer than those for Al−O.[33,34] Furthermore, for each of the Me^{2+} ions examined, the calculated Me−O bond distances are considerably longer than the Al−O in the host AlPO framework, showing that when a Me^{2+} ion substitutes for Al^{3+} in the AlPO framework, the dopant introduces a structural strain. This factor may contribute to limiting the maximum level of doping achievable experimentally to a low value or a few atomic percent.

When comparing the Me−O bond distances calculated in our work with the experimental values, we notice that the error is not uniform; the calculated Me−O distance for Mg, Ni, and Zn ions, which are stable only in the 2+ oxidation state, is within the experimental error of ±0.02 Å associated with the EXAFS technique employed. Our calculated bond distances for Mn and Co ions, which are known experimentally to exist in both +2 and +3 oxidation states in the AlPO framework, instead, show a much larger difference from the experimental results, up to 0.06 Å for Mn.

It is significant that the calculated values are always greater than the experimental ones. Our calculations correspond to a calcined form of the MeAlPO framework, in which no template molecule is present in the structure and all of the dopants are in the reduced 2+ oxidation state. The experimental measurements concerning the reduced form of the MeAlPO catalyst are often performed on the as synthesized material, whereas calcination to remove the organic template can in fact oxidize, at least partially, the Me dopants. The overestimation of the calculated, compared to the experimental, bond distance of Mn^{II} and Co^{II} ions suggests that, in the as-synthesized MeAlPO structure, some of the dopant ions may be present in 3+ oxidation state, so that a mixture of Me^{II} and Me^{III} is present in the framework. Because the XAS data are element-specific, but cannot differentiate its oxidation state,[35] the experimental results represent an average of the properties of all the Me dopants present in the solid. A fraction of Me ions in 3+ oxidation state will cause a decrease of the Me-O bond distances observed experimentally, proportional to the fraction of Me ions oxidized in the real material. Results of calculations similar to those reported here can effectively help to determine the average oxidation state of the transition metal dopants in the catalysts, such as the MnAlPO materials discussed in reference 36.

Let us now consider the changes that occur in the T−O−P framework angles in the doped MeAlPO frameworks. From the value of the Me−O−P and T−O−P angles, we can obtain information on the structural distortion around the metal dopant, complementary to the Me-O bond distances examined above. The deviation of the calculated T−O−P angles between the doped and the undoped AlPO structure, in fact, provides a fast way to estimate the range of the structural distortion around the metal dopant. A graphical representation of the relaxation around the dopant is provided in Figure 2; let us first imagine that, upon inclusion in the AlPO framework of the Me^{2+} dopant, only its nearest neighbor oxygens are allowed to relax around the metal dopant, whereas the next-nearest neighbor phosphorus

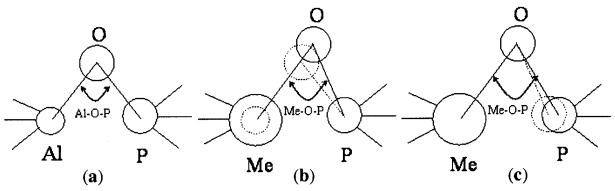

Figure 2. Graphical representation of the relaxation around the metal dopant and its effects on the Me−O−P angles.

ions and the rest of the structure are kept fixed (Figure 2b). The larger the size of the metal dopant, the more its nearest neighbor oxygens will relax away from it. This relaxation movement causes a decrease of the Me−O−P angles compared to the original Al−O−P; the bigger the structural relaxation upon doping, the larger the change of the Me−O−P angle. In addition to the presence of the large metal dopant, we have seen in the previous discussion that the Me−O_H bond of the dopant to the protonated oxygen is longer than the other Me−O bonds. Therefore, we expect the Me−O_H−P angle centered on the bridging hydroxyl group to be particularly small.

Of course, the real situation is more complex, and the structural relaxation will extend beyond the first shell of neighbors around the metal dopant. A radial relaxation of the next-nearest neighbor phosphorus ions away from the Me center, which is expected to follow the relaxation of the nearest neighbor oxygens, will cause the Me−O−P angle to increase. As the relaxation extends to further shells of ions in the structure, also the P−O−Al angles centered on oxygens further away from Me will vary. However, because the crystalline matrix exerts a steric constraint on the metal dopant, the extent of structural relaxation decays when moving away from the dopant ion. The change in the bond angles between undoped and doped materials provides a numerical way to estimate the range of this structural relaxation: monitoring the change in the calculated T−O−P bond angles for subsequent shells of neighbors, will enable us to estimate quickly the region of the solid that is structurally affected by the dopant. Furthermore, it has been shown that the ^{31}P NMR chemical shift, i.e., a measurable observable, correlates with the average T−O−P bond angle in AlPOs.[37] Understanding the correlation between the properties of the metal dopant, such as charge and ionic radius, with the local and long-ranged structural relaxation in a simple polymorph (AlPO-34), and in an idealized situation of noninteracting defect centers, will therefore provide a valuable reference against which to compare and rationalize the experimental information obtained for real MeAlPO catalysts.

The calculated values of the T−O−P angles (T = Me and Al) for subsequent shells of neighbors of the metal dopants are reported in Table 2. Indeed, we find that the distortion from the undoped material is particularly pronounced around the protonated oxygen (column Me−O_H−P), whose angle with the framework ions changes as much as 30° for the large Sr^{2+} ion. The difference from the undoped framework is important for all of the four nearest-neighbor oxygens of the dopant (column Me-O_{nn}-P), as expected from the description given in Figure 2. The local distortion causes a decrease of the T−O−P angle averaged over the whole structure (which is the value measured experimentally by ^{31}P NMR). When we limit our attention to the oxygens that are not nearest neighbor of the dopant (column Al−O−P in Table 2), however, we notice only minor changes (of less than 1°) from the undoped AlPO-34 framework structure. This result suggests that the structural distortion caused by the dopant is "local", and affects its nearest nighbour ions, but does not propagate to the undoped regions of the framework.

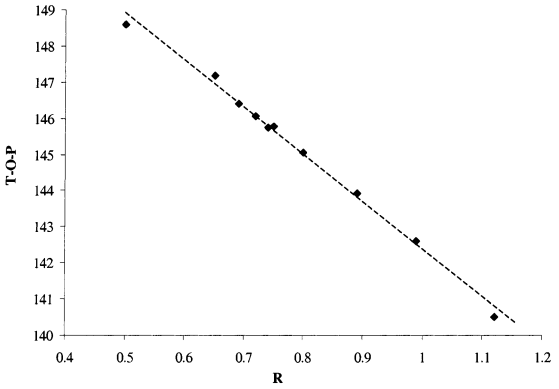

Figure 3. Calculated T−O−P angle (in degrees) as a function of the ionic radius R of the Me dopant (from ref 28). R is given in Å.

TABLE 3: Mulliken Population Analysis of the Electronic Distribution around the Me Dopants in MeAlPO-34[a]

Me^{II}	Q(Me)	$Q(O_{1-3})$	$Q(O_H)$	$Q(O_{1-4})$	q_b(Me−O)
Mg	1.67	−1.26	−1.03	−1.20	0.052
Ca	1.78	−1.25	−1.01	−1.19	0.002
Cr	1.60	−1.22	−0.98	−1.17	0.045
Mn	1.54	−1.21	−0.99	−1.16	0.053
Fe	1.62	−1.24	−1.01	−1.18	0.064
Co	1.61	−1.24	−1.01	−1.18	0.070
Ni	1.85	−1.32	−1.03	−1.24	−0.012
Zn	1.42	−1.20	−0.98	−1.15	0.091
Sr	1.84	−1.25	−1.01	−1.19	−0.019

[a] The symbol Q refers to the net ionic charges on the metal dopant and oxygens; $Q(O_{1-3})$ is the average net charge of the three unprotonated oxygens that are nearest neighbor to the Metal dopant; $Q(O_H)$ refers to the charge of the protonated oxygen, q_b denotes the bond population, in |e|.

The only exceptions to the above result are Ca and Sr, i.e., the largest dopant ions examined (see the Me-O bond distances in Table 1). The optimized value of the Al−O−P bond angles away from the Ca and Sr dopants are lower than the value of the Al−O−P angle in the undoped AlPO-34, which indicates that the structural strain caused by the biggest dopant ions is long-ranged and propagates toward the undoped regions of the host framework. In Figure 3, we plot the calculated value of the T−O−P angle as a function of the ionic radius of the dopant. These two observables show a good linear correlation, clearly indicating that the structural distortion correlates with the steric hindrance of the large divalent ions when they are isomorphously introduced in the AlPO framework.

3.2. Electronic Properties of Dopants. Let us now consider the bonding between the divalent metal dopants and the neighboring oxygens in the framework. To this purpose, we shall use results from a Mulliken population analysis of the electronic distribution, reported in Table 3, and electron and spin density plots, shown in Figures 4 and 5.

We see in Table 3 that the values of the overlap population q_b(Me−O) are low, which suggests that the nature of bonding between the Me dopants and the neighboring oxygen atoms is ionic in nature. The same situation is observed for the original metal ion Al, which is found to be of ionic nature in AlPOs.[22,25] To support this finding, in Figure 4, we show the electron density maps (obtained as the difference between the electron density in the solid and the superposition of isolated formal ions) for the Me−O bond in the metal-doped AlPO framework. The maps are drawn in a plane which contains the 2+ metal dopant, the oxygen bonded to the charge compensating proton, and the next nearest phosphorus ion bonded to the oxygen of the figure. From the electron density plots, we clearly see an electronic

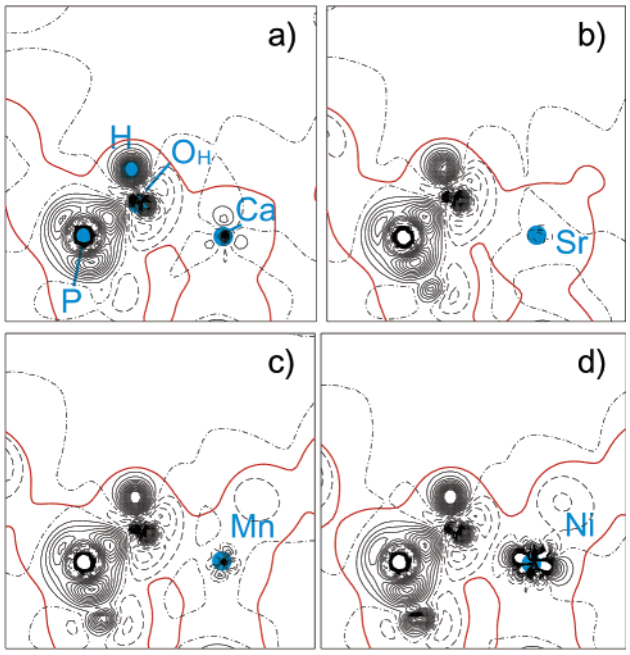

Figure 4. Difference electron density maps (solid minus isolated formal ions), plotted in a plane containing one (a) Ca−O(H)−P, (b) Sr−O(H)−P, (c) Mn−O(H)−P, or (d) Ni−O(H)−P unit in AlPO-34. Continuous and dashed lines correspond to positive and negative densities, plotted between −0.1 and +0.1 au (|e| $bohr^{-3}$) at linear steps of 0.01 au. The red line is the total electron density level of 0.01 au and indicates the framework size.

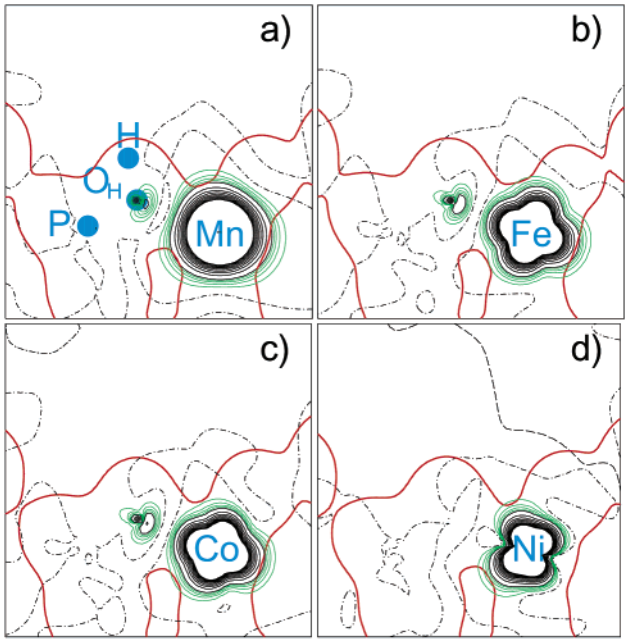

Figure 5. Spin electron density maps, plotted in a plane containing one (a) Mn−O(H)−P, (b) Fe−O(H)−P, (c) Co−O(H)−P, and (d) Ni−O(H)-P unit. Continuous and dashed black and green lines are the isodensity levels calculated from the spin density; the black lines correspond to the spin levels between −0.1and +0.1 a.u (|e| $bohr^{-3}$) at steps of 0.01, and the green lines correspond to spin levels between 0 and 0.005 au at steps of 0.001. The red line is the total electron density level of 0.01 au and indicates the framework size.

redistribution in the covalent P−O bonds but only minor features around the metal dopants. We can therefore describe the bonding between the metal dopant and the oxygens as being ionic, while the bonding between phosphorus and oxygen is covalent.

For the original AlPO-34 framework, experimental evidence shows that Al is capable of increasing reversibly its coordination number when Lewis bases such as water and ammonia are present in the cages.[38,39] Furthermore, TGA data on doped AlPO materials show that the hydrophilicity of the framework increases when dopant ions are incorporated,[40,41] a result that is consistent with the ionic nature of the Me-O bonding found in our calculations. Ionic bonds are in fact nondirectional and more flexible than covalent bonds toward changes of the coordination number. During adsorption processes, the dopant ions can act as Lewis acid centers, able to increase their coordination in the presence of Lewis bases.

To investigate further the Lewis acidity, we have calculated the spin electron density of the open shell transition metal dopants Mn^{2+}, Co^{2+}, Fe^{2+}, and Ni^{2+} in their equilibrium structure; the results are plotted in Figure 5, where the continuous and dashed black and green lines are the isodensity levels calculated from the spin density.

The interstitial space within the microporous framework is not all accessible to adsorbed molecules: the Pauli repulsion caused by the overlap between the electronic density of the adsorbed molecule and of the framework atoms renders the adsorption process energetically unfavorable when the molecules become too close to the framework atoms. How close the adsorbed molecule can approach the framework and its active site depends on the radial extent of the electronic density of the MeAlPO host framework; the red line in Figure 5 is the isodensity level of 0.01 au, which appears to represent an effective framework size, beyond which adsorbed molecules cannot approach the framework ions.

For open shell transition metal ions in a high spin state, the spin density represents the distribution of the half filled d AOs of the metal dopant. All of the ions reported in Figure 5 have at least 5 d electrons. The spin density represents in this case the d orbitals responsible for the Lewis acidity, which are half filled, whereas the remaining levels are completely occupied by two electrons and, hence, inactive for Lewis acidity.

We clearly see in Figure 5 that the half-filled orbitals are well localized on the transition metal ions, with only minor contributions on the framework oxygen and Phosphorus ions, in agreement with the ionic description of the Me−O bonding discussed earlier. Furthermore, the orientation of the spin density differs according to the electronic configuration of the dopant ion. As a result, the extent of spin density that spills outside the Pauli repulsion area (red line) varies considerably among the dopants examined. In particular, for the Ni^{2+} ion, the Lewis-active orbitals are oriented along the framework; a molecule inside the microporous cages of a Ni-doped AlPO will therefore encounter Pauli repulsion from the framework before having an effective interaction with the Lewis active orbitals of the Ni ion, which is not the case, instead, for Mn, Fe, and Co dopant ions, whose spin density spills outside the Pauli repulsion area. Lewis base molecules in Fe-, Co-, and Mn-doped materials can therefore undergo an appreciable chemical interaction with the Lewis acid center before being repelled by the framework. Our finding concerning the lack of Lewis acidity of Ni doped AlPO frameworks is supported by experimental evidence. Lischke et al reported that NiAlPO-5 has a lower concentration of Lewis acid sites[42] than most other MeAlPOs (Me: Cr, Co, Mg, Mn, Co, and Si).

We further see in Figure 5 that the spilling of the spin density outside the Pauli repulsion area is more effective on the side of the framework opposite to the proton. The interaction of Lewis basic molecules with the Lewis active center appears therefore to be more effective when the molecule can approach the metal center from the side opposite to the protonated oxygen, which is indirectly confirmed by experimental work on Co^{2+}-doped AlPOs,[9] in which the authors found that an effective Lewis interaction between the framework Co^{2+} and acetonitrile can only take place when the $Co-O_H$ bond of Co^{2+} with the Brønsted acid OH group is broken. This structural property of Lewis-type interactions can differentiate the Lewis acidity of different AlPO frameworks. We expect low-valent transition metal dopants to be more Lewis active when they are located in open regions of framework, where the space behind the dopant and the protonated oxygen is not protected by other ions of the framework. The structures are instead expected to be less Lewis active when the dopant and the protonated oxygen cannot be approached from behind by adsorbate molecules, which can be the case when the transition metal dopant is situated in 1-dimensional channels built up only of double-walled structural units, such as the double-4 or double-6 ring cages found in AlPO5.

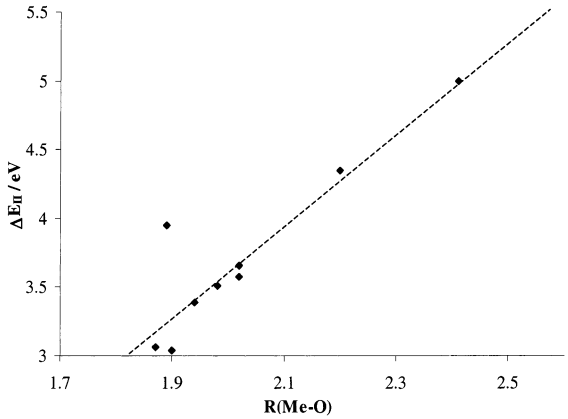

Figure 6. Calculated replacement energy ΔE_{II} for the dopants examined, as a function of the metal -oxygen bond distance, R(Me−O), in Å.

TABLE 4: Calculated Replacement Energy ΔE_{II} (in eV) of a Framework Al with Me^{2+} Dopants, According to Equation (2) in the Text

Sr	Zn	Ni	Co	Fe	Mn	Cr	Ca	Mg	Me
ΔE_{II}	5.00	3.04	3.95	3.39	3.51	3.66	3.58	4.35	3.07

3.3. Substitutional Energy of a Framework Al with Me^{2+} Dopants. The values of the replacement energy ΔE_{II} of a framework Al^{3+} with Me^{2+} dopants, calculated according to eq 2 are summarized in Table 4, whereas Figure 6 presents a plot of the calculated values of ΔE_{II} for the different dopant ions examined, as a function of the Me−O bond distance in the optimized MeAlPO-34 structure. We clearly see from the Figure 6, that the replacement energy increases linearly as a function of the Me−O bond distance; the larger the size of the metal dopant, the more energetically unstable its inclusion in the AlPO framework. The only exception to the linearity of ΔE_{II} as a function of the ionic size is Ni^{2+}, whose replacement energy is $\sim$ 0.9 eV higher than expected from its ionic radius. The latter result is due to the instability of Ni^{2+} in tetrahedral coordination. The crystal field stabilization energy of octahedral and tetrahedral Ni^{2+} has been estimated for oxides with the spinel structure;[43] the resulting values are 1.23 eV for octahedral Ni^{2+} and 0.37 eV for tetrahedral Ni^{II}, with a difference of 0.86 eV. This value is close to the energy difference of $\sim$ 0.9 eV, required in our calculations for bringing the replacement energy ΔE_{II} of Ni^{2+} in AlPO-34 in line with the trend observed for the other Me^{2+} dopants.

Our calculations predict therefore a marked preference of Ni^{2+} for octahedral coordination in the AlPO-34 framework; we expect the substitution of Ni^{2+} in the tetrahedral sites to be unstable and difficult to achieve experimentally. Our finding is consistent with experimental evidence, which shows that the amount of nickel that can be incorporated into the AlPO framework is relatively low compared to other divalent metal ions.[44]

In light of the results described in section 3.1 and in particular from the linear relationship between the size of the metal dopant and the structural distortion it causes in the AlPO framework (see Figures 3), we attribute the increasing value of ΔE_{II} as a function of the Me−O bond distance shown in Figure 6 to the larger distortion of the framework, required to accommodate the larger dopant ion.

From the relatively large values of ΔE_{II}, we can infer a general thermodynamic instability of the doped AlPO framework, a result supported by experimental evidence, which shows that AlPO frameworks are unstable upon high metal doping.

3.4. Catalytic Activity. The catalytic activity of zeotypes in dehydration and isomerization reactions is connected to the presence of acid sites in the molecular sieve structure. For example, the activity and selectivity within a series of ZSM-5 catalysts were found to be a function of the total acidity of the zeolite:[45] On reducing the concentration of acid sites in MeAlPOs catalysts, the conversion of olefins to paraffins decreases,[46,47] whereas moderate acid sites are more selective in the skeletal isomerization of alkenes.[42]Apart from the bridging hydroxyl groups of the framework, responsible for the Brønsted acidity, the Lewis acidity of transition metal dopants, discussed in section 3.3, can also contribute to the total acidity of the MeAlPO catalysts. However, Thomas[48] reported strong evidence to show that the catalytic activity of MeAlPO's is directly proportional to the concentration of Brønsted acid sites, and it does not correlate with the concentration of the Lewis acid sites. Mastering the Brønsted acidity conferred to the MeAlPO framework by the isomorphous inclusion of different low-valent dopant ions is therefore a topic of crucial importance in understanding the catalytic function of these materials.

Attempts have been made to correlate experimentally the acid strength of MeAlPOs to different structural parameters related to the Me dopant, such as the ionic radius of the metal[49] or the Me−O−P bond angle.[16,18] Hočevar et al.,[49] for instance, reported a correlation between the acid strength and the Me−O bond distance in the MeAlPO catalysts: the smaller the size of the metal dopant, the stronger the Brønsted acidity. The same authors also concluded that the acid strength of MeAlPO catalysts depends only on the *type* of metal incorporated into the framework and not on the structural type of the AlPO framework. Other authors, instead, assumed a correlation of the acidity with the electronic properties of the Metal dopant, such as its electronegativity.[17]

We have seen in section 3.1 that a close correlation exists between the different structural parameters; we shall now investigate if the results of our computational work support a correlation of the acid strength with any of the structural or electronic properties of the Me dopants proposed in the experimental literature.

To investigate the acid properties of MeAlPOs, we have calculated the OH stretching frequency of the Brønsted acid site for each divalent dopant examined in AlPO-34. The OH stretching frequency is an effective measure of the chemical strength of the OH bond and is often assumed to correlate with its acidity.

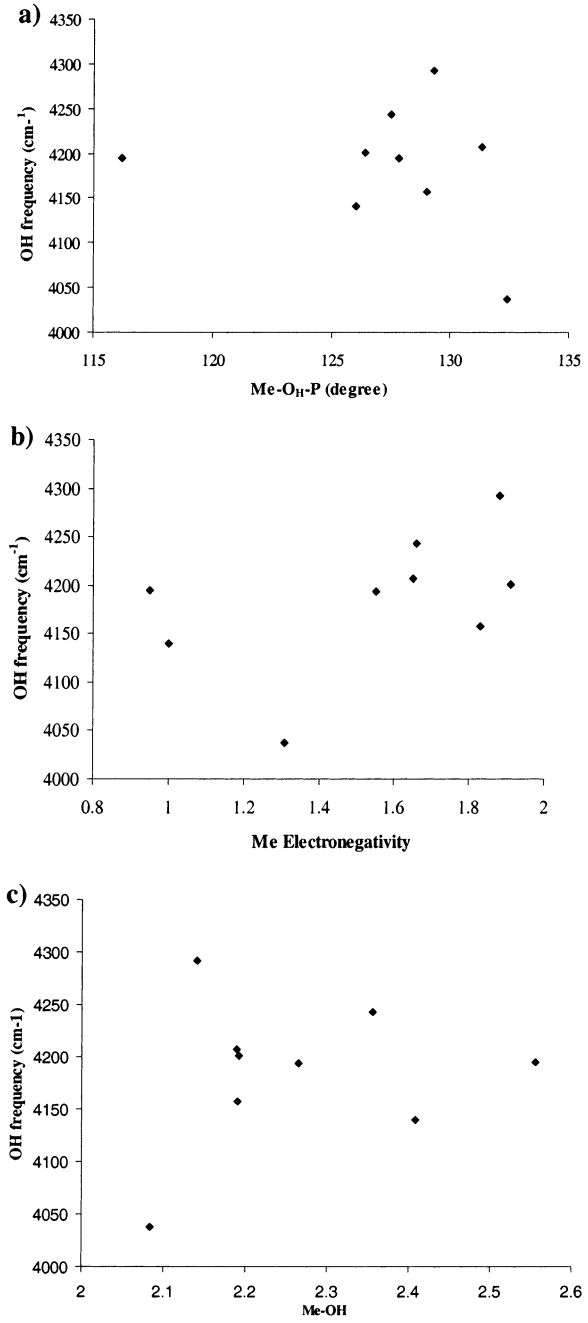

Figure 7. Calculated ν_{OH} stretching frequencies (cm^{-1}) of the Brønsted acid site, as a function of (a) Me−O−P angle (b) electronegativity of the dopant (from ref 28), and (c) the Me−O_H bond distance.

For each metal examined, we have calculated the phonon spectrum in the Γ point of reciprocal space for the equilibrium structure and in the harmonic approximation, from which we derived the OH stretching frequency ν_{OH}. In Figure 7, we report plots of the calculated ν_{OH} as a function of the three parameters described above; R(Me−O_H), the Me−O_H−P angle, and the electronegativity of the metal dopant. In none of these cases were we able to identify an absolute correlation. Because the equilibrium local structure of the Brønsted OH group is very dissimilar among the dopant ions examined, correlating the acid properties with a single structural parameter related to the chemical nature of the dopant does not appear to be satisfactory. Subsets of dopants do exist, whose acid strength correlates with the chemical nature of the dopant; however, extension of the study to a wider range of low-valent dopant ions shows that the correlation within the subsets is fortuitous and not the result

of a law with general validity. Our results do not therefore support a simple correlation between the acid strength of doped zeolites and AlPOs with either ionic radius, electronegativity, or bond angles proposed in the literature.

Our calculations predict the acidity to decrease in the order of MgAlPO ≫ FeAlPO > CoAlPO > MnAlPO > ZnAlPO > NiAlPO > CrAlPO. The Mg doped AlPO framework has the strongest acid sites, whereas CrAlPO is the weakest acid.

In light of the calculated values of ν_{OH}, we expect Cr, Ni, and Zn dopants in AlPO-34 to yield the highest selectivity, whereas MgAlPO will be more active at the expense of selectivity. Linshke et al.[42] reported that MgAlPO-5 has the lowest catalytic activity for the conversion of methanol to light olefins, when compared with other MeAlPO-5 materials, (Me = Cr, Zr, Co, and Ni). The low activity of MgAlPO, however, is due to the fast formation of coke precursor compounds on the active sites of the catalyst in early stages of the chemical reaction, which suggests that Mg-doped AlPOs indeed have very strong acid sites. MnAlPO-5 and CoAlPO-5 are initially highly active and selective; their catalytic activity and selectivity is lost rather quickly during the catalytic reaction. This is thought to be due to the fact that CoAlPO-5 and MnAlPO-5 catalysts have a higher concentration of strong Lewis acid sites. Ni AlPO was claimed to have the highest selectivity and stability. Our results indicate that Ni in AlPO frameworks has moderate Brønsted acidity and weak or no Lewis acidity, confirming the experimental hypothesis.

It is finally of interest to compare our results with the work of Nur and Hamdan,[16] who examined the selective conversion of cyclohexanol over different MeAlPO-5 catalysts. The experimental work found that the acidity of MeAlPO-5 catalysts correlates with the ionic size of the Me dopant ions, according to the following order: Mn > Zn > Co > Mg, i.e., the bigger the size of the metal dopant, the stronger its acidity. In addition the authors report that the T−O−P bond angle, measured by ^{31}P MAS NMR spectra, increases with the ionic size of the metal dopant and that the lattice parameter of the MeAlPO-5 catalysts decreases with increasing the dopant content. None of the above results agrees with our calculations, and the result reported in ref 16 concerning the volume per formula unit of the doped materials, i.e., that the volume decreases on incorporating large metal dopants in the framework, is at least counter-intuitive. We consider the discrepancy between our work and the results of ref 16 to be due to the interaction of dopant ions in the framework of the experimental catalysts. Although our model of the solid accounts for the behavior of isolated dopant ions and applies to AlPO frameworks with a low content of dopant ions, the catalysts employed by Nur and Hamdan contained a large fraction (∼10%) of low-valent ions. In such a case, the formation of clusters of dopant ions in a limited region of the framework is very likely; we consider that the interaction between defect centers can cause the different structural behavior observed in reference 16 and modify the catalytic activity of the solid. Indeed, the concentration of dopant ions is an important feature of the catalyst that needs proper investigation both in computational and experimental work.

4. Conclusion

We have studied, using periodic ab initio QM methods, the structure and acidity of divalent metal ions in the AlPO-34 framework. From the results of our calculations and comparison with experiment, we conclude the following points:

(1) The local envoriment of divalent dopants is a distorted tetrahedron, in which the Me−O_H bond of the dopant to the protonated oxygen is ∼0.15 Å longer than the other three Me−O bonds.

(2) The deviation of the calculated T−O−P angles between the doped and the undoped AlPO structure provides a way of estimating the range of the structural distortion around the metal dopant. The structural strain is local for small ions, whereas for bigger dopants, it propagates further away toward the undoped regions of the host AlPO framework.

(3) The nature of bonding between the Me^{2+} dopants and the neighboring oxygen atoms is ionic in nature; the ionicity of the Me−O bonds explains the Lewis acidity of the Me^{2+} ions, which are able to increase their coordination number in the presence of Lewis bases. For the Ni^{2+} ion, however, the Lewis active orbitals are oriented within the framework, where they are screened from an effective Lewis-type interaction with adsorbed molecules. The attack of Lewis bases is favored from the side of the framework opposite to the Brønsted acid proton.

(4) The replacement energy of a framework Al^{3+} with a Me^{2+} ion increases linearly as a function of the ionic size of the Me^{2+} ions and of the Me−O bond distance: the larger the size of the metal dopant, the more difficult its inclusion in the AlPO framework. The Ni^{2+} ion is unstable in tetrahedral sites due to crystal field effects, and therefore inclusion of Ni in AlPOs is expected to be difficult to achieve experimentally.

(5) The acid strength is due to a complex combination of the structural and electronic features of the dopant ion and does not show appreciable correlation with the local environment or electronic distribution of the Metal dopant in the framework.

Acknowledgment. We are grateful to Dr. G. Sankar and Dr. M. Alfredsson for useful discussions. We thank EPSRC for funding this research via a studentship to I.S. and one Advanced Fellowship to F.C. The Royal Society is gratefully acknowledged for funding the computational resources employed.

Supporting Information Available: Previously unpublished basis set used for Sr^{2+}. This information is available free of charge via the Internet at http://pubs.acs.org.

References and Notes

(1) Thomas, J. M.; Thomas, W. J. *Principles and Practice of Heterogeneous Catalysis*; VCH: Weinheim, Germany, 1996.
(2) Sankar, G.; Raja, R.; Thomas, J. M. *Catal. Lett.* **1998**, *55*, 15.
(3) Weisz, P. B. *Pure Appl. Chem.* **1980**, *52*, 2091.
(4) Weisz, P. B.; Haag, W. O.; Lago, R. M. *Nature* **1984**, *309*, 589.
(5) Lewis, D. W.; Sankar, G.; Wyles, J. K.; Thomas, J. M.; Catlow, C. R. A.; Willock, D. J. *Angew. Chem.-Int.* **1997**, *36*, 2675.
(6) Catlow, C. R. A.; Ackermann, L.; Bell, R. G.; Corà, F.; Gay, D. H.; Nygren, M. A.; Pereira, J. C.; Sastre, G.; Slater, B.; Sinclair, P. E. *Faraday Discuss* **1997**, *106*, 1.
(7) Draznieks, C. M.; Newsam, J. M.; Gorman, A. M.; Freeman, C. M.; Ferey, G. *Angew. Chem. Int. Ed.* **2000**, *39*, 2770.
(8) Hartmann, M.; Kevan, L. *Chem. Rev.* **1999**, *99*, 635.
(9) Barrett, P. A.; Sankar, G.; Catlow, C. R. A.; Thomas, J. M. *J. Phys. Chem. Sol.* **1995**, *6*, 1395.
(10) Raja, R.; Sankar, G.; Thomas, J. M. *Chem. Commun.* **1999**, *9*, 829.
(11) Sheldon, R. A.; Arends, I. W. C. E.; Lempers, H. E. B. *Colle. Czech. Chem. Commun.* **1998**, *63*, 1724.
(12) Barrett, P. A.; Sankar, G.; Jones, R. H.; Catlow, C. R. A.; Thomas, J. M. *J. Phys. Chem. B* **1997**, *101*, 9555.
(13) Thomas, J. M. *Sci. Am.* **1992**, *286*, 82.
(14) Thomas, J. M. *Angew. Chem. Int. Ed.* **1999**, *38*, 3588.
(15) Corma, A. *Catal Today* **1997**, *38*, 257.
(16) Nur, H.; Hamdan, H. *Matt. Res. Bull* **2001**, *36*, 315.
(17) de las Pozas, C.; lopez-Cordero, R.; Gonzales-Morales, J. A.; Travieso, N.; Roque-Malherbe, R. *J. Mol. Catal* **1993**, *83*, 145.
(18) Rabo, J. A.; Gajda, G. J. *Catal. Rev. Sci. Eng.* **1989**, *31*, 385.
(19) Sheldon, R. A.; Kochi, J. K. *Metal catalyzed Oxidations of Organic compounds*; Academic Press: New York, 1981.

(20) Saadoune, I.; Corà, F.; Alfredsson, M.; Catlow, C. R. A. *J. Phys. Chem.* **2003**, *107*, 3012.
(21) Saunders, V. R.; Dovesi, R.; Roetti, C.; Causà, M.; Harrison, N. M.; Orlando, R.; Zicovich-Wilson, C.; Doll, K.; Civalleri, B. *CRYSTAL 2001 User's Manual*; University of Torino: Turin, Italy, 2001.
(22) Corà, F.; Catlow, C. R. A. *J. Phys. Chem. B* **2001**, *105*, 10278.
(23) www.chimifm.unito.it/teorica/crystal/Basis_Sets/mendel.html.
(24) Dovesi, R. Private communication.
(25) Corà, F.; Catlow, C. R. A.; D'Ercole, A. *J. Mol. Catal. A* **2001**, *166*, 87.
(26) Sankar, G.; Thomas, J. M. *Top. Catal.* **1999**, *8*, 1.
(27) Gale, J. D.; Henson, N. J. *J. Chem. Soc. Faraday Trans.* **1994**, *90*, 3175.
(28) Lide, D. R., Ed.; *CRC Handbook of Chemistry and Physics*, 75th ed.; CRC Press: Boca Raton, FL, 1994.
(29) Doll, K.; Saunders, V. R.; Harrison, N. M. *J. Quantum Chem.* **2001**, *82*, 1.
(30) Civalleri, B.; D'Arco, Ph.; Orlando, R.; Saunders, V. R.; Dovesi, R. *Chem. Phys. Lett.* **2001**, *348*, 131.
(31) Chen, J. S.; Thomas, J. M.; Sankar, G. *J. Chem. Soc. Faraday Trans.* **1994**, *90*, 3455.
(32) Lok, B. M.; Messina, C. A.; Patton, R. L.; Gajek, R. T.; Cannan, T. R.; Flanigen, E. M. *J. Am. Chem. Soc.* **1984**, *106*, 6092.
(33) Nicholas, J. B. *Top. Catal.* **1997**, *4*, 157.
(34) Sauer, J. in *Modelling of structure and reactivity in Zeolites;* Catlow, C. R. A., Ed.; Academic Press: London, 1992; p 183.
(35) Sankar, G.; Thomas, J. M.; Catlow, C. R. A. *Top. Catal.* **2000**, *10*, 255.
(36) Corà, F.; Sankar, G.; Catlow, C. R. A.; Thomas, J. M. *Chem. Commun.* **2002**, 734.
(37) Müller, D.; Jahn, E.; Ladwig, G.; Haubenreisser, U. *Chem. Phys. Lett.* **1984**, *109*, 332.
(38) Tuel, A.; Caldarelli, S.; Meden, A.; McCusker, L. B.; Baerlocher, C.; Ristic, A.; Rajic, N.; Mali, G.; Kaucic, V. *J. Phys. Chem. B* **2000**, *104*, 5697.
(39) Peeters, M. P. J.; Van de Ven, L. J. M.; de Haan, J. W.; Van Hooff, J. H. C. *J. Phys. Chem.* **1993**, *97*, 8254.
(40) Jänchen, J.; Peeters, M. P. J.; Van Wolput, J. H. M. C.; Wolthuizen, J. P.; Van Hooff, J. H. C. *J. Chem. Soc. Faraday Trans.* **1994**, *90*, 1033.
(41) Zenonos, C.; Sankar, G.; Corà, F.; Lewis, D. W.; Pankhurst, Q. A.; Catlow, C. R. A.; Thomas, J. M. *Phys. Chem. Chem. Phys.* **2002**, *4*, 5421.
(42) Lischke, G.; Parlitz, B.; Lohse, U.; Schreier, E.; Fricke, R. *App. Catal. A: General* **1998**, *166*, 351.
(43) West, A. R. *Basic Solid State Chemistry*; Wiley: Chichester, U.K., 1988.
(44) Hartmann, M.; Kevan, L. *Chem. Rev.* **1999**, *99*, 635.
(45) Gayubo, A. G.; Benito, P. L.; Aguayo, A. T.; Olazar, M.; Bilbao, J. *J. Chem. Technol. Biotechnol.* **1996**, *65*, 186.
(46) Froment, G. F.; Dehertog, W. J. H.; Marchi, A. J. *Catalysis* **1992**, *9*, 1.
(47) Stöcker, M. *Microp. Mesop. Mater.* **1999**, *29*, 3.
(48) Thomas, J. M. *Angew Chem-Int.* **1999**, *38*, 3588.
(49) Hočevar, S.; Batista, J.; Kaučič, V. *J. Catal.* **1993**, *139*, 351.
(50) Sankar, G.; Gleeson, D.; Thomas, J. M.; Smith, A. D. *J. Syn. Rad.* **2001**, *8*, 625.
(51) Barett, P. A.; Sankar, G.; Catlow, C. R. A.; Thomas, J. M. *J. Phys. Chem.* **1996**, *100*, 897.
(52) Xu, Y.; Couves, J. W.; Jones, R. H.; Catlow, C. R. A.; Greaves, G. N.; Chen, J.; Thomas, J. M. *J. Phys. Chem. Sol.* **1991**, *10*, 1229.
(53) Tusar, N. N.; Tuel, A.; Arcone, I.; Kaucic, V. *Prog. Zeolites Microporous Materials* **1997**, *105*, 501.
(54) Thong, N.; Schwarzenbach, D. *Acta Cryst. A* **1979**, *35*, 658.